ELSEVIER

Int. J. Therm. Sci. 41 (2002) 163–172

International Journal of Thermal Sciences

Heat transfer measurements for smooth and rough tilted semi-cylindrical cavities

Walid Chakroun *, Mir Mujtaba A. Quadri

Center of Research for Experimental Thermal Sciences, Mechanical Engineering Department, College of Engineering and Petroleum, Kuwait University, P.O. Box 5969, Safat 13060, Kuwait

Received 29 November 2000; accepted 12 March 2001

Abstract

This paper presents the effect of roughness on heat transfer for semi-cylindrical cavity. Heat transfer measurements are performed on smooth and rough surfaces for different tilt angles. The results are compared with a rectangular cavity of the same surface area to study the effect of cavity shape on heat transfer. The roughness composed of 0.002 m diameter rods installed along the length of the cavity at equal spacing. Roughness shows a large effect on heat transfer for the semi-cylindrical cavities. Two competing effects are present with the existence of roughness. Roughness may increase the blockage effect on the flow that can cause the buoyancy force to decrease, but on the other hand it increases the turbulence intensity resulting in a higher heat transfer. Both effects are function of tilt angles. Heat transfer for the cylindrical cavity is higher than the rectangular cavity for all tilt angles. This increase in heat transfer for the cylindrical cavity is due to the absence of sharp corners that can slow the buoyancy driven convection mechanism. © 2002 Éditions scientifiques et médicales Elsevier SAS. All rights reserved.

Keywords: Heat transfer; Rectangular cavity; Semi-cylindrical cavity; Roughness

1. Introduction

Natural convection in open cavities are getting more attention due to the importance of such geometry in solar thermal central receiver system, where heat losses affect the performance of the system. Further, applications of cavities include aircraft-brake housing system, pipes connecting reservoirs of fluids with different temperatures, refrigerators, fire research, electronic cooling, energy-saving household refrigerators, waste heat disposal, building, insulation, micro-electronic equipment, and many others.

Both experimental and numerical studies have been carried out with various fluids and different heating wall conditions.

Experimental and numerical works were carried out to better understand the heat transfer mechanism inside cavity. The effect of aspect ratio ($AR = H/B$) and opening ratio ($OR = a/H$) as shown in Fig. 1 was investigated experimentally at different tilt angles for rectangular cavities [5,11]. Problems involving natural convection in open cavities were also studied by Doria [9] in predicting fire spread in a room and Jacobs et al. [15,16] in modeling circulation above street and geothermal reservoirs. Experimental studies were performed by Chen et al. [7] and Sernas and Kyriakides [23]

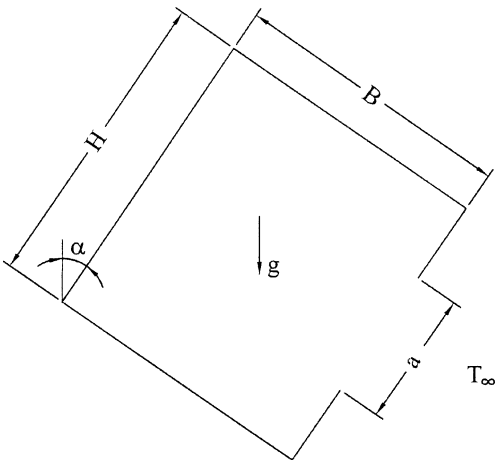

Fig. 1. Geometry of a partially open rectangular cavity.

* Correspondence and reprints.
E-mail address: chakroun@kuc01.kuniv.edu.kw (W. Chakroun).

1290-0729/02/$ – see front matter © 2002 Éditions scientifiques et médicales Elsevier SAS. All rights reserved.
PII: S1290-0729(01)01294-7

Nomenclature

a	height of aperture	m
AR	cavity aspect ratio $= H/B$	
B	Height of the cavity walls	m
d	distance from the centerline of the opening to the base of the cavity	m
DR	opening displacement ratio $= d/H$	
F_{pa}	configuration factor between hot cavity surface and the aperture	
Gr_L	Grashof number for cavity with isothermal walls	
Gr_L^*	Grashof number for cavity with walls having constant heat flux	
g	acceleration due to gravity	$m{\cdot}s^{-2}$
h	local value of heat transfer coefficient	$W{\cdot}m^{-2}{\cdot}K^{-1}$
$\overline{h}$	average convective heat transfer coefficient	$W{\cdot}m^{-2}{\cdot}K^{-1}$
H	width of the cavity	m
I	electric current	Ampere
k	thermal conductivity of air	$W{\cdot}m^{-1}{\cdot}K^{-1}$
k_w	thermal conductivity of the aluminum	$W{\cdot}m^{-1}{\cdot}K^{-1}$
k_{in}	thermal conductivity of the hard insulation (polystyrene)	$W{\cdot}m^{-1}{\cdot}K^{-1}$
L	length of the cavity	m
L_c	characteristic length of the cavity, also the length of the cavity	m
$\overline{Nu}$	average Nusselt number	
$\Delta\overline{Nu}$	uncertainty in $\overline{Nu}$	
$(\Delta\overline{Nu})_p$	precision limit error in $\overline{Nu}$	
$(\Delta\overline{Nu})_b$	bias limit error in the variable $\overline{Nu}$	
OR	opening ratio $= a/H$	
q''	heat flux at the cavity surface $= IV$	$W{\cdot}m^{-2}$
q''_c	convective heat transfer rate per unit area of the cavity surface	$W{\cdot}m^{-2}$
q''_{cd}	conductive heat loss rate through the insulation	$W{\cdot}m^{-2}$
q''_r	radiation heat loss rate per unit area of the cavity surface	$W{\cdot}m^{-2}$
R	radius of the semi-cylindrical cavity	m
s	distance along a wall	m
r_i	inner radius of the hard insulation on the semi-cylindrical cavity	m
r_o	outer radius of the hard insulation on the semi-cylindrical cavity	m
T	Temperature	K
T_i	inner surface temperature of the hard insulation	K
T_o	outer surface temperature of the hard insulation	K
$\overline{T}_w$	average cavity surface temperature	K
$\overline{T}_{w_i}$	local section cavity surface temperature	K
T_∞	ambient temperature	K
V	voltage	volts
x	one of the variables used in the determination of $\overline{Nu}$	
Δx_{b_i}	bias limit error in the variables x_i	
Δx_{p_i}	precision limit error in the variables x_i	

Greek symbols

α	tilt angle of cavity, positive direction in clockwise direction (see Fig.1)	
β	coefficient of thermal expansion of air	K^{-1}
ε	emissivity of the cavity surface	
ν	kinematic viscosity of air	$m^2{\cdot}s^{-1}$
σ	Stefan Boltzmann constant	$W{\cdot}m^{-2}{\cdot}K^{-4}$

in modeling solar receivers. Also, Showole and Tarasuk [24] have done experimental studies on natural convection in inclined cavities. They concluded that upward-faced cavities enhance heat transfer while downward-faced cavities tend to suppress the buoyancy mechanism. Also they concluded that the lower corners that exist between the base and the side walls of the cavity alter the growing boundary layer pattern observed in on a flat plate and cause the heat transfer rate to drop.

Most of the previous works in this area were focussed on smooth-wall enclosures. Due to surface corrugation or mounting of circuit chips, the walls of the enclosures could be considered rough. Ruhul Amin [21] studied the effect of placing adiabatic roughness elements at the bottom of an enclosure cooled at the top and heated at the bottom. He found that the presence of roughness elements on the hot horizontal wall increases heat transfer rate across the enclosure in comparison with a corresponding smooth walled enclosure. Also he concluded that in some cases of the smooth walled enclosure has more heat transfer rate than a rough wall, since the rough wall delays the onset of convection motion.

Most of the previous studies were carried out on rectangular cavities with different heating wall configurations and at different inclination angles. In [4,25] presented numerical studies of natural convection in cylindrical cavity. Different boundary conditions were looked at to predict the thermal performance for storage tanks. The effect of aspect ratio on cylindrical cavity was studied by [14,22]. The authors are not aware of any experimental studies on semi-cylindrical cavity.

The present work focusses on the study of natural convection from semi-cylindrical cavities at different tilt angles. Semi-cylindrical cavities can be found in many engineering applications. Semi-cylindrical cavites can be used in the design of solar thermal receiver systems, where heat loss affects the performance of the system.

Table 1
Review of previous work on fully/partially open cavities

Reference		Geometry		*DR*	B.C.*	α	*Pr*	*Gr* or *Ra*
		AR	*OR*					
Le Quere et al.	[17]	1	1	0.5	*A*	0, 20, 45	0.73	$10^4 \leqslant Gr_L \leqslant 10^7$
		0.5, 2	1	0.5	*A*	0	0.73	$Gr_L = 10^7$
Penot	[20]	1	1	0.5	*A*	0, ±45, 90	0.7	$10^3 \leqslant Gr_L \leqslant 10^7$
Miyamoto	[19]	1	0.5, 1	0.5	*A*	$-45 \leqslant \alpha \leqslant 80$	0.7	$7 \times 10^3 \leqslant Ra_B \leqslant 7 \times 10^4$
		1	0.5, 1	0.5	*A*	0	0.7	$1 \leqslant Ra_B \leqslant 7 \times 10^5$
Showole and Tarasuk	[24]	0.25, 0.5, 1	1	0.5	*A*	$-90 \leqslant \alpha \leqslant -30$	0.7	$10^4 < Ra_L < 5 \times 10^5$
		1	1	0.5	*A*	−90, −45	0.7	$10^3 < Ra_L < 5 \times 10^5$
Angirasa et al.	[2]	1	1	0.5	*A*	0	0.7	$10^4 \leqslant Gr_L \leqslant 10^7$
Sernas and Kyriakides	[23]	1	1	0.5	*B*	0	0.7	$Gr_L = 10^7$
Hess and Henz	[13]	1	0.5, 1	0.5	*C*	0	7	$3 \times 10^{10} \leqslant Ra_L \leqslant 2 \times 10^{11}$
Chan and Tien	[6]	1, 0.143	1	0.5	*C*	0	1.7	$10^3 \leqslant Ra_L \leqslant 10^7$
Angirasa et al.	[1]	1	1	0.5	*C*	0	$0.1 < Pr < 1$	$10^2 \leqslant Ra_L \leqslant 10^8$
Lin and Xin	[18]	1	1	0.5	*C*	0	0.7	$Ra_L = 10^{10}, 10^{11}$
Chakroun et al.	[5]	0.25, 0.5, 1	0.25, 0.5, 1	0.5	*E*	$-90 \leqslant \alpha \leqslant 90$	0.7	$Gr_L^* = 5.5 \times 10^8$
Elsayed et al.	[11]	1	1	0.5	*C*	0	0.71	$10^2 \leqslant Gr_L \leqslant 10^5$
Elsayed	[10]	1	1	0.5	*D*	0	0.72	$Gr_L = 10^5, 10^7, 10^{10}$
Present		Semi-cylindrical cavity			*F*	$-90 \leqslant \alpha \leqslant 90$	0.7	$Gr_L^* = 5.5 \times 10^8$

* see Table 2 explanation.

The flow induced by buoyancy-driven heat transfer mechanism is totally different in both semi-cylindrical and rectangular cavities. Sharp corners effect in rectangular cavity was studied by many researchers [25]. They show a significant effect of the sharp corners on the flow field and heat transfer process in the open-ended cavity via vorticity generation and the introduction of flow instability. The previous finding has motivated the present work where in a semi-cylindrical surface, obviously no sharp corners are present. Both rectangular and semi-cylindrical cavities with the same surface area are tested under the same boundary condition to better understand the effect of the cavity geometry.

The effect of roughness in semi-cylindrical cavity is another objective of this paper. This paper provides heat transfer results for two semi-cylindrical cavities one with smooth wall and the other one with a periodic array of 0.002 m diameter rods mounted on otherwise smooth wall. The 0.002 m rods are distributed 0.05 m apart. Transient as well as steady state values of Nusselt number at different tilt angles are presented.

Roughness in forced convection is proven to be a good technique to increase the heat transfer mechanism. However, in free convection blockage effect induced by the existence of rough surface is essential since the convection mechanism is weaker than that of forced convection. Two competing effects are present with the existence of roughness. Roughness produces drag causing blockage effect to take place resulting in a less heat transfer. Roughness also increases the turbulent intensity on the surface, which causes heat transfer to increase. The magnitude of each effect is a function of tilt angle.

A brief review of the previous work on fully and partially open rectangular cavities is summarized in Table 1. Four types of boundary conditions are included in the review.

Table 2
Explanation for the types of boundary conditions given in Table 1

B. C. type	Boundary conditions on walls			
	1	2	3	4
A	T_h	T_h	T_h	T_h
B	T_h	T_h	T_∞	*N/A*
C	T_h	*a*	*a*	*a*
D	T_c	*a*	*a*	*a*
E	q''	*a*	*a*	*a*
F	q''	q''	q''	q''

T_h—constant wall temperature, $T_c < T_\infty < T_h$, q''—constant heat flux on the wall, *a*—adiabatic, *N/A*—not applicable.

Different types of boundary conditions on the walls of the cavity are explained in Table 2. In Table 1 two types of Grashof numbers are used, one when the cavity walls are maintained at constant temperature (isothermal walls) and the other when the cavity walls has constant heat flux. These tables are taken from Ref. [11] for comparison.

2. Experimental setup

The schematic diagram of the experimental setup is shown in Fig. 2. The cavity is mounted on a stand and supported by two arms. The arms and the stand are designed to minimize the disturbance to the airflow and to ensure good physical stability. The cavity can be rotated about its longitudinal axis. The angle of rotation was measured with respect to the vertical axis and can be read from a protractor. Two types of cavities of same surface area, a rectangular and a semi-cylindrical shape are used in this study.

Fig. 3 shows the cross section of both cavities. The semi-cylindrical cavity is made up of aluminium. The cavity has

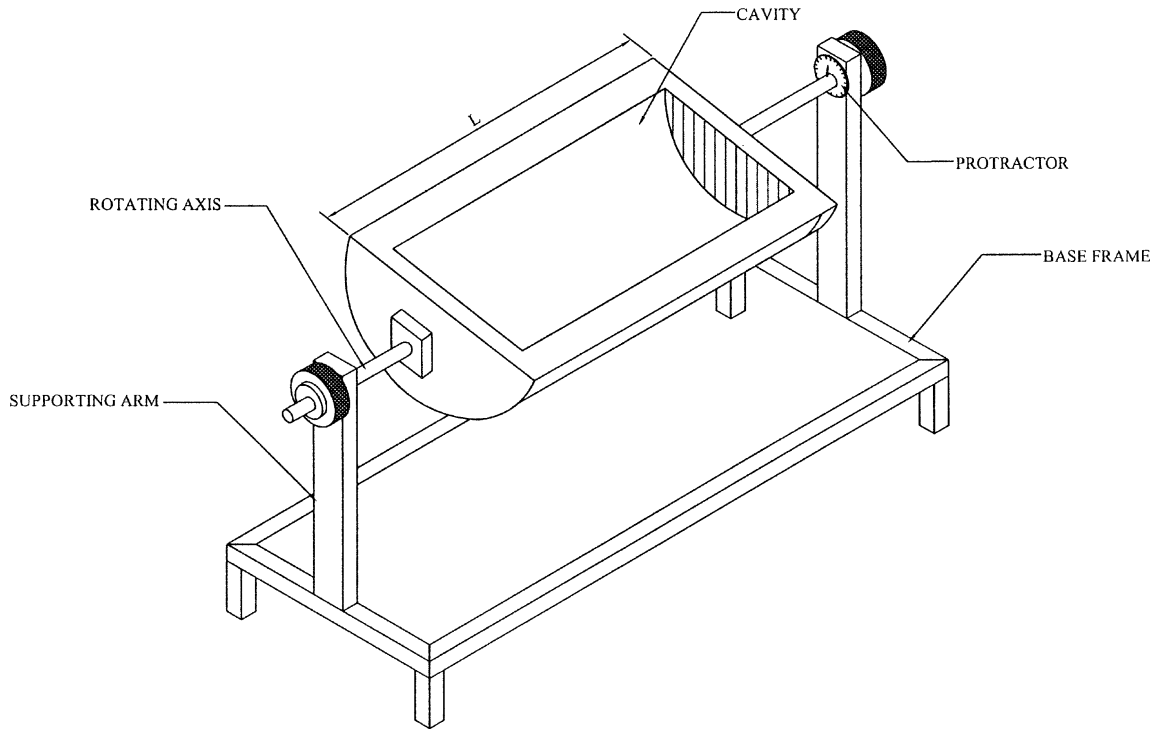

Fig. 2. Main features of the experimental setup.

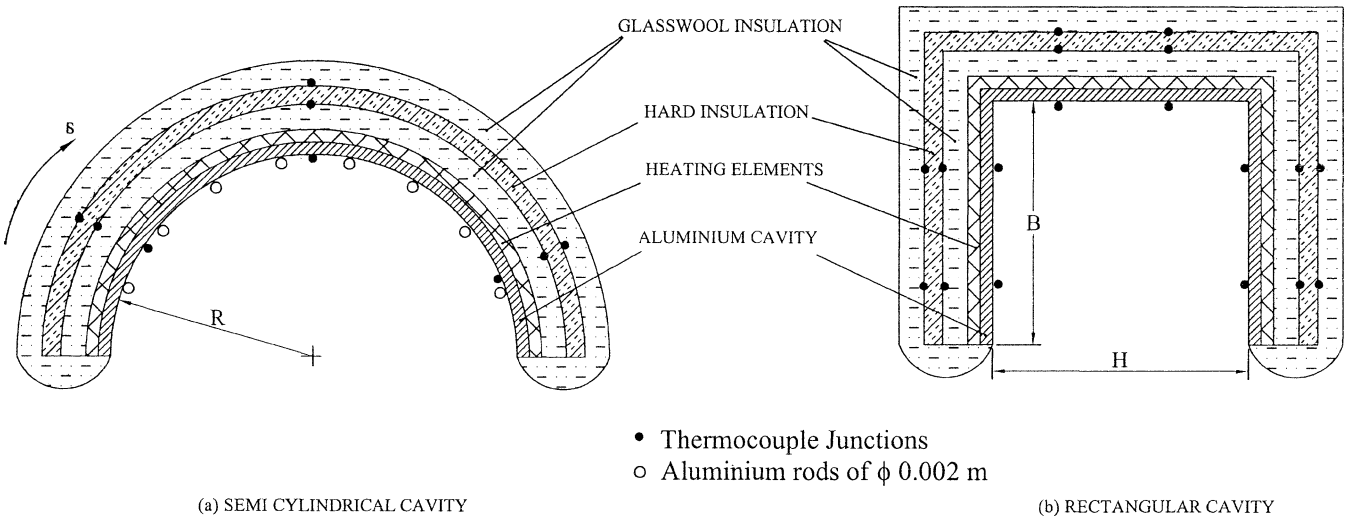

Fig. 3. Cross-section of the cavities with thermocouple locations.

a radius (R) of 0.15 m and a length (L) of 0.9 m. The length of the cavity was chosen to ensure two-dimensional flow of air inside the cavity. The thickness of the cavity sheet is 0.004 m. The cavity is heated electrically with flexible silicone rubber heater. A total of nine heating pads were used, each producing a maximum of 7750 $W{\cdot}m^{-2}$. The pads are self adhesive, and were fixed to the back of the cavity. The heating pads are covered with glass wool insulation of 0.02 m thickness followed by a layer of 0.03 m thick hard polystyrene insulation. Another layer of 0.02 m glass wool insulation is placed on the top. The cylindrical cavity is closed at the ends by plexiglass plate of 0.009 m thickness, the outer surface of which is covered by 0.02 m layer of glass wool (see Fig. 3(a)).

The rough semi-cylindrical cavity composed of 0.002 m diameter aluminium rods placed 0.05 m apart along the cavity length as shown in Fig. 3(a). The rods are fixed to the surface such that they are in full contact with the surface along the cavity.

The design of the rectangular cavity is shown in Fig. 3(b). The rectangular cavity has a cross section of 0.147 m × 0.158 m and a length of 0.915 m. The cavity surface is made up of aluminium of 0.004 m thickness and it is closed from the ends with plexiglass sheets. Similar heating

elements as mentiond above are used to heat the surface of the rectangular cavity. Heating pads, insulation type and thickness are arranged similarly in both cavities.

The heat input to the heating pads was controlled by an electric circuit of a 240 V and 50 Hz power supply and a voltage regulator. The output of the voltage regulator was directly coupled to the heating pads. All pads are connected in parallel, hence they receive the same power. The voltage and current supplied to the pads are measured with a digital multimeter with an accuracy of 0.025%. The power supplied to the pads was calculated from the voltage and the current.

The temperatures were monitored with the help of 30 (semi-cylindrical cavity) and 55 (rectangular cavity) copper-constantan thermocouples. Eleven and eighteen thermocouples were fixed to the surface of the semi-cylindrical cavity and the rectangular cavity, respectively. One thermocouple was used to measure the ambient temperature and the rest to measure the temperature across the hard insulation. The temperatures across the insulation were used to calculate the conduction heat loss. Thermocouples are placed at three equally spaced sections along the length of the cavity as shown in Fig. 3. All the thermocouples are connected to a digital temperature recorder (Make: Omega, Model: DR231) which in-turn is connected to a computer to record the data continuously as a function of time. A recording time of 10 hours, with a period of 15 min was used to record the temperature history until steady state is achieved. The face of the cavity was inclined at 13 different tilt angles from 90° (cavity facing down) to −90° (cavity facing up) by an increment of 15°.

3. Nusselt number data reduction equation

The average Nusselt number from the cylindrical cavity is defined as

$$\overline{Nu} = \frac{\bar{h}R}{k} \tag{1}$$

where $\bar{h}$ is the average heat transfer coefficient between the cavity and the surroundings, R is the radius of the cavity ($R = B$ for rectangular cavity), and k is the thermal conductivity of air in the cavity. In terms of the local heat transfer coefficient h, Eq. (1) is rewritten in the following form:

$$\overline{Nu} = \frac{1}{k}\frac{R}{H}\int_0^H h\,\mathrm{d}s \tag{2}$$

where $H = \pi R$ and s is defined as shown in Fig. 3. When the cavity surface is heated at constant heat flux, the local heat transfer coefficient is given by the equation

$$h = \frac{q_c''}{(T_w - T_\infty)} \tag{3}$$

where T_w is the local temperature of the cavity surface and q_c'' is the convective heat transfer rate per unit area of the cavity surface. Dividing the wall into five equal sections, Eqs. (2) and (3) can be combined to give

$$\overline{Nu} = \frac{R}{5k}\sum_{i=1}^{5}\frac{q_c''}{(T_{w_i} - T_\infty)} \tag{4}$$

where i is the order of the various sections on the heated surface.

To calculate q_c'', an average energy balance for the heated plate gives

$$IV = HL\left(q_c'' + q_{cd}'' + q_r''\right) \tag{5}$$

Where V and I are the voltage and the current to the heating elements, respectively, q_{cd}'' is the conduction heat lost through the insulation to ambient, and q_r'' is the heat transferred by radiation from the cavity surface to the surroundings. The double prime indicates that the heat transfer term is per unit area of the cavity surface.

The radiation heat loss q_r'' from the hot surface is estimated as follows:

$$q_r'' = \sigma\left[\left(\overline{T}_w + 273\right)^4 - (T_\infty + 273)^4\right]\left(\frac{1-\varepsilon}{\varepsilon} + \frac{1}{F_{pa}}\right)^{-1} \tag{6}$$

where $\overline{T}_w$ is the average temperature of the cavity surface, ε is its emissivity and F_{pa} is the configuration factor between the plate and the aperture. In Eq. (6) it is assumed that the surrounding is a black body at temperature T_∞. The configuration factor F_{pa} is calculated from the analytical expression given by Gross et al. [12].

The conduction heat loss q_{cd}'' in Eq. (4) is the heat loss through hard wall insulation. This is expressed as follows:

$$q_{cd}'' = \frac{k_{in}}{R}\frac{(T_i - T_o)}{\mathrm{Ln}(r_o/r_i)} \quad \text{for cylindrical cavity} \tag{7}$$

where k_{in} is the thermal conductivity of the hard insulation, T_i and T_o is the average inner and outside surface temperatures of the hard wall insulation, respectively.

The conduction heat loss q_{cd}'' for a rectangular cavity is the sum of the heat loss through all hard insulation walls. This is expressed as follows:

$$q_{cd}'' = \frac{k_{in}}{H}\sum_{j=1}^{3}(T_{j,i} - T_{j,o}) \tag{8}$$

where j is the wall identification number.

Using Eqs. (6) and (7), the expression of $\overline{Nu}$ given Eq. (2) yields

$$\overline{Nu} = \frac{R}{5k}\sum_{i=1}^{5}\left\{\frac{IV}{HL} - \frac{k_{in}}{R}\frac{(T_i - T_o)}{\mathrm{Ln}(T_i/T_o)} - \sigma\left[\left(\overline{T}_w + 273\right)^4 - (T_\infty + 273)^4\right]\left(\frac{1-\varepsilon}{\varepsilon}\right)^{-1} + \frac{1}{F_{pa}}\right\} \tag{9}$$

The Grashof number for cavity with isothermal walls is defined as follows:

$$Gr_L = g\beta\frac{|T_w - T_\infty|L_c^3}{\nu^2} \tag{10}$$

where L_c is a characteristic length of the cavity (R for semi-cylindrical cavity and H for rectangular cavity) and T_w is the temperature of the cavity surface.

The Grashof number for cavities with constant heat flux is defined as

$$Gr_L^* = g\beta \frac{q'' L_c^4}{k\nu^2} \tag{11}$$

where $q'' = IV$, is the heat flux applied at the cavity surface. The data in this paper are presented for $Gr_L^* = 5.5 \times 10^8$.

Uncertainty analysis

The uncertainty in the Nusselt number determined experimentally was estimated based on the ANSI/ASME Standard on Measurement Uncertainty [3] using the procedure of Coleman and Steele [8]. The uncertainty $\Delta\overline{Nu}$ in the value of $\overline{Nu}$ is expressed as follows:

$$\Delta\overline{Nu} = \sqrt{\left(\Delta\overline{Nu}\right)_b^2 + \left(\Delta\overline{Nu}\right)_p^2} \tag{12}$$

where the subscripts b and p refer, respectively to bias and precision limit errors.

The values of $(\Delta\overline{Nu})_p$ and $(\Delta\overline{Nu})_b$ are then determined as follows:

$$(\Delta Nu)_p^2 = \sum_{i=1}^{n} \left(\frac{\partial \overline{Nu}}{\partial x_i} \Delta x_{p_i} \right)^2 \tag{13}$$

$$\left(\Delta\overline{Nu}\right)_b^2 = \sum_{i=1}^{n} \left(\frac{\partial \overline{Nu}}{\partial x_i} \Delta x_{b_i} \right)^2 + 2\left(\frac{\partial \overline{Nu}}{\partial x_i} \right)\left(\frac{\partial \overline{Nu}}{\partial x_j} \right) \overline{\Delta x_{b_i} \Delta x_{b_j}} + \cdots \tag{14}$$

Δx_{b_i} is the bias limit error in the each variable x_i that effect the determination of $\overline{Nu}$, and $\overline{\Delta x_{b_i} \Delta x_{b_j}}$ is the correlated bias error for variables x_i and x_j.

The values of Δx_{b_i} and Δx_{p_i} of the various variables used in the determination of $\overline{Nu}$ are given in Table 3. Only the bias limit errors of temperature readings are correlated with each other since the same thermocouple wires were used to measure all the temperatures. The value of $\overline{\Delta x_{b_i} \Delta x_{b_j}}$ for all temperatures was taken equal to 0.18 °C.

Table 3
Precision and bias limit errors for the variables used in the determination of $\overline{Nu}$

Variable	Δx_{p_i}	Δx_{b_i}
Current	0.23%	0.2%
Volt	0.5%	0.3%
Temperature (any)	0.1 °C	0.23 °C
Distance (any)	0	0.03 mm
Thermal conductivity of air	0	0.5%
Thermal conductivity of the plexiglass	3%	3%
Emmisivity of aluminium	0	10%

It was found that the uncertainty $\Delta\overline{Nu}$, for the data of $\overline{Nu}$ which will be reported later in the following section, ranges from four percent to ten percent depending on the type of cavity and the tilt angle α.

4. Results and discussion

The results in this study are presented for both rectangular and semi-cylindrical cavities. Two semi-cylindrical cavities were tested one with smooth wall and the other with a periodic array of 0.002 m diameter rods mounted on otherwise smooth surface. The 0.002 m rods are distributed 0.05 m apart. Transient as well as steady state average Nusselt numbers are reported at different inclination angles for the semi-cylindrical cavity. Steady state Nusselt number is also reported for the rectangular cavity. Both rectangular and semi-cylindrical cavities were designed to have the same convection surface area. Therefore, the difference in the average Nusselt number from case to case and from angle to angle is due solely to the convection mechanism and the change in the shape of the cavity and not due to the increase in surface area. Also the same heat flux was maintained on the surface for all three cases for easy comparison. All the data were collected at Grashof number, $Gr_L^* = 5.5 \times 10^8$.

Figs. 4–10 present the time history of average Nusselt number for the smooth and rough semi-cylindrical cavities at different tilt angles. Fig. 4 presents the transient Nusselt number at angle of 90°. At angle of 90°, the opening of the cavity is facing down where the buoyancy force is suppressed, allowing heat to be transferred only by molecular conduction through the air enclosed within the cavity. After the steady state time has surpassed, the air is

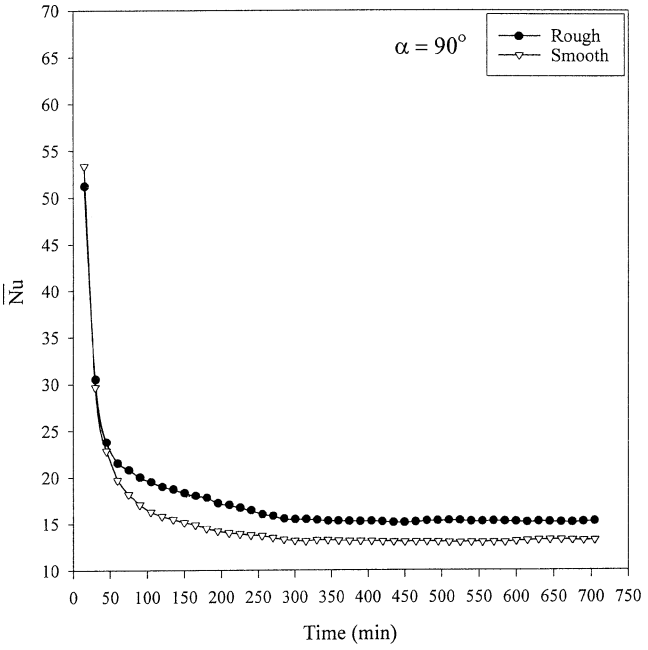

Fig. 4. Time history for average Nusselt number for the tilt angle of 90°.

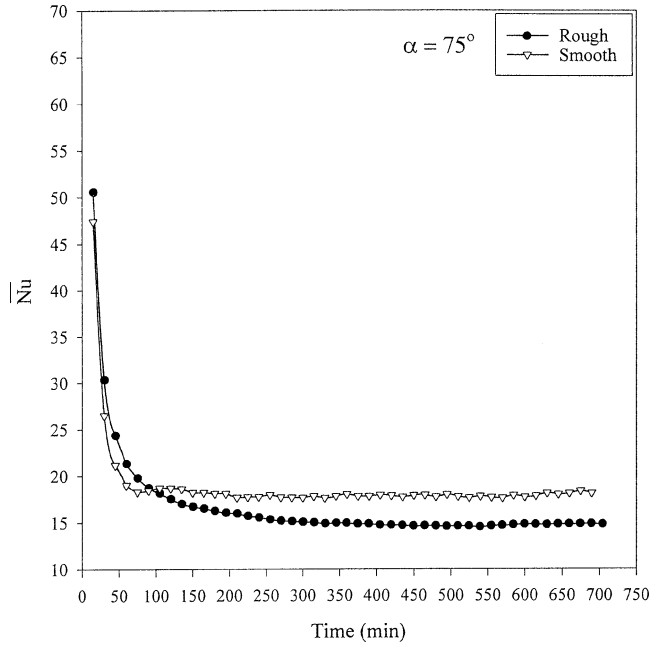

Fig. 5. Time history for average Nusselt number for the tilt angle of 75°.

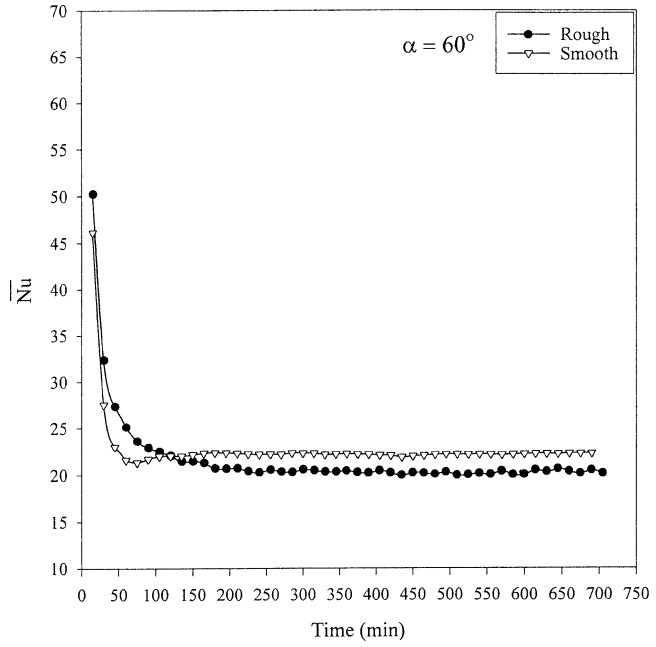

Fig. 6. Time history for average Nusselt number for the tilt angle of 60°.

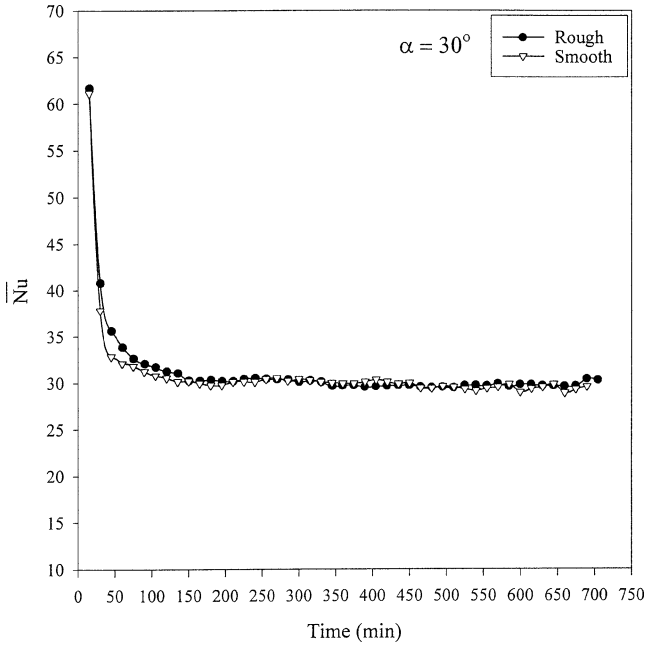

Fig. 7. Time history for average Nusselt number for the tilt angle of 30°.

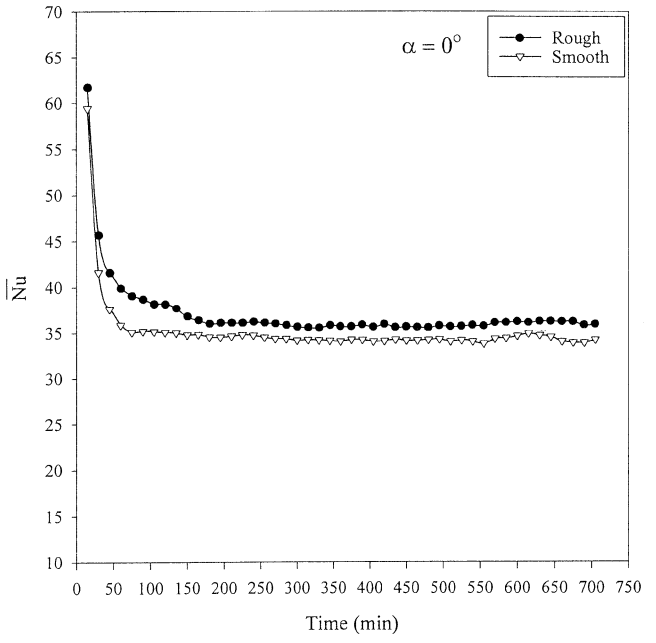

Fig. 8. Time history for average Nusselt number for the tilt angle of 0°.

stratified inside the cavity. The rough wall shows higher value for the average Nusselt number than that of smooth wall and this is due mainly to the increase in surface area that is estimated to be 6%. No convection is taken place at this tilt angle, therefore the roughness here has no effect on the behavior of the flow inside the cavity. At this angle Nusselt number reveals to have the lowest value.

At other tilt angles, roughness appears to have a large effect on heat transfer inside the cavity. Two competing effects are present with the existence of roughness. Roughness produces drag causing blockage effect to take place resulting in a less heat transfer. Roughness also increases the turbulent intensity on the surface, which causes heat transfer to increase. The contribution of each effect is a function of tilt angle.

Figs. 5–7 present the time history for both rough and smooth semi-cylindrical cavities at angles of 75°, 60°and 30° degrees respectively. For angles of 75° and 60°, the buoyancy driven force is still weak. The drag produced by the presence of roughness, is slowing down the onset of convection and the smooth wall shows larger values for the

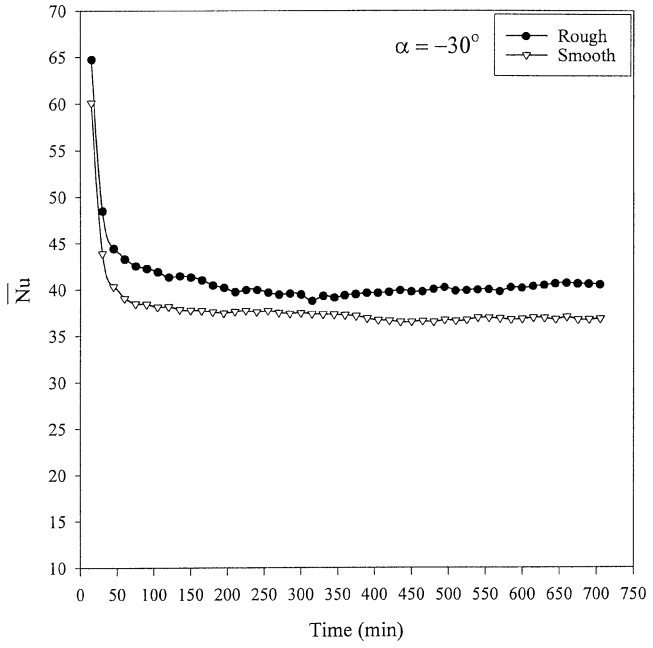

Fig. 9. Time history for average Nusselt number for the tilt angle of −30°.

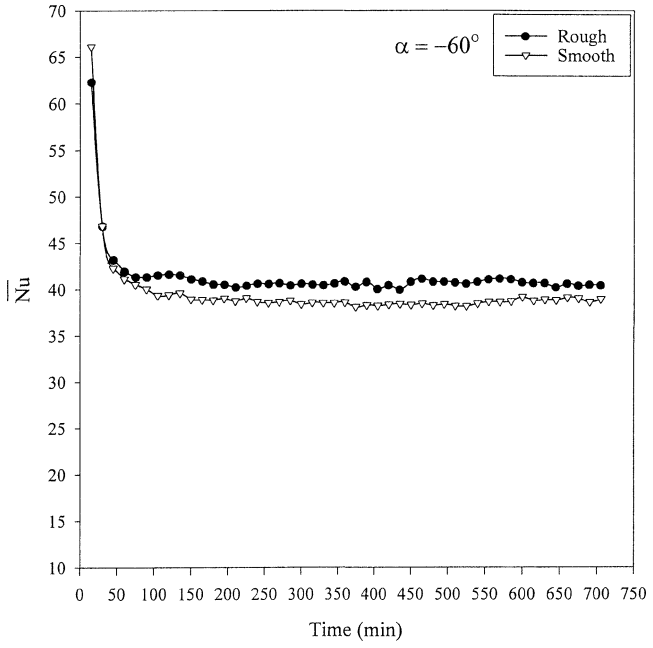

Fig. 10. Time history for average Nusselt number for the tilt angle of −60°.

heat transfer over that of the rough wall. The buoyancy-driven flow gets stronger as the inclination angle increases. The stronger the buoyancy force, the larger is the effect of turbulence induced by roughness. The increase in convection mechanism seems to overcome the drag produced by the presence of roughness for angle 30°, and Nusselt number seems to be the same for both rough and smooth surfaces. At this angle, the figure reveals that both blockage effect and more turbulence to the flow induced by roughness have the same contribution. Both effects cancel each other and no net effect on heat transfer is observed.

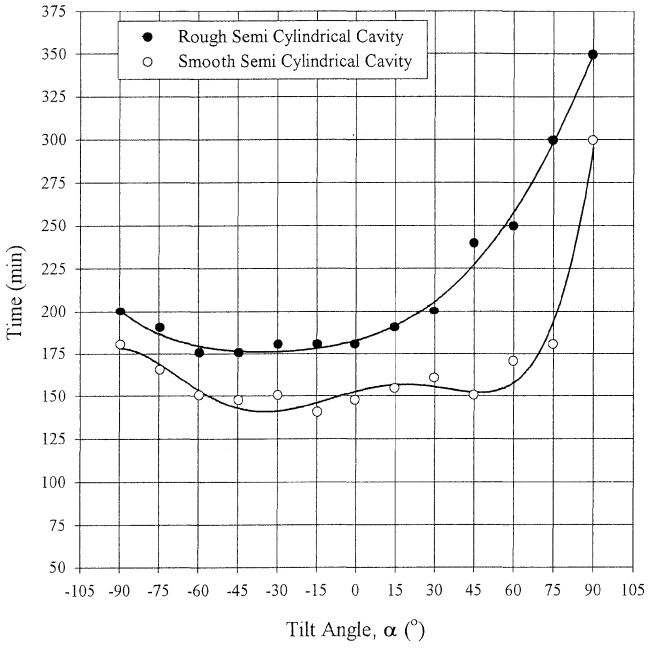

Fig. 11. Effect of tilt angle on time required to achieve steady state for semi-cylindrical cavity.

Figs. 8–10 present the time history for the average Nusselt number at inclination angle of 0°, −30°, and −60°, respectively. The buoyancy mechanism is strong for this range of inclination angle. Roughness causes the heat transfer to increase over that of the smooth surface for this range of inclination angle. The increase in turbulent intensity caused by the presence of roughness causes the boundary layer on the surface to trip and more turbulence and mixing is introduced in the flow resulting in increase in heat transfer.

The height of the roughness elements compared to the boundary layer thickness is an important factor in the effect of roughness. If the roughness height is within the viscous sub-layer, the viscous effect dominates and the flow behaves as if the wall is smooth. In fully-rough flows, the roughness effects dominate, and viscosity is no longer important. Transitionally-rough flows are those in between where both viscous and roughness effects are important.

Fig. 11 presents the time required to achieve steady state for both smooth and rough semi-cylindrical cavities. Steady state is recorded when the average Nusselt number remains constant for at least 120 minutes. The figure reveals that the rough cases require more time to achieve steady state than those of smooth cases. For the smooth case the steady state time is almost constant between −90° and 45° and increases sharply for the rest of the angles. For the rough cavity, the steady state time remains almost the same for −90° to 0° and increases sharply for 0° to 90°. When the cavities are facing down more time is required to achieve steady state.

Fig. 12 presents the steady state Nusselt number for the rectangular cavity and for both smooth and rough semi-

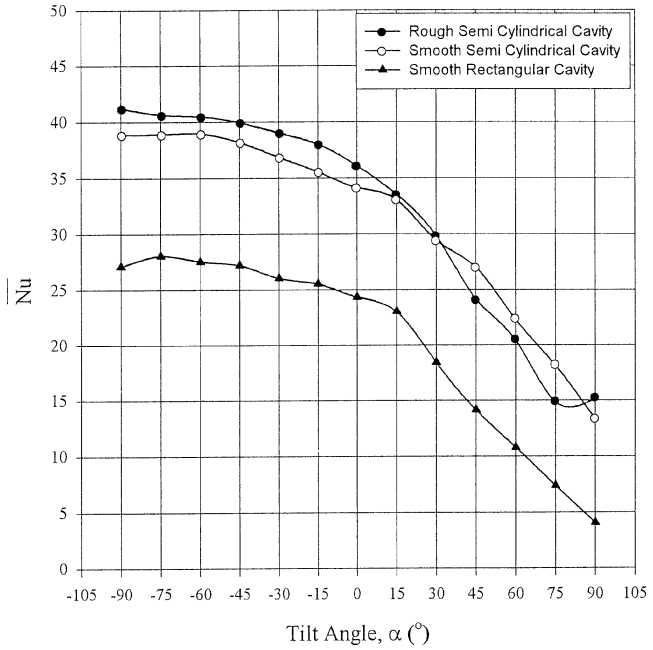

Fig. 12. Effect of tilt angle on the average Nusselt number for semi-cylindrical and rectangular cavities.

cylindrical cavities. The average Nusselt number is plotted as a function of tilt angle. The square cavity shows lower values for Nusselt number than that of semi-cylindrical cavity. The heat transfer mechanism is different for each geometry, even though the three cases have the same surface area and same heat flux. The increase in heat transfer for the smooth cylindrical cavity over the square cavity ranges from 50 to 200% and depends on the tilt angle. Lesser values for the heat transfer for the rectangular cavity is believed to be caused by the presence of sharp corners. Sharp corner effects via vorticity generation and flow instability are not present in the cylindrical cavity. The flow motion inside the semi-cylindrical cavity seems to be more stable and oriented properly allowing the flow to move faster. The lower corners which exist between the base and the side walls of the cavity in the rectangular case alter the growing boundary layer pattern and cause the heat transfer rate to drop.

Nusselt number for all three cases seems to be minimum at angle of 90°. As mentioned before, at this angle the cavity is facing down and the heat is transferred through molecular conduction. Nusselt number for the rectangular cavity is about 4.5 compared to 13 for the semi-cylindrical smooth case. The initial inclination of the cavity from 90° to −15° causes a significant increase in average heat transfer rate, but a further increase in inclination angle appears to cause a small increase in average heat transfer rate. Comparison is better made when the range of inclination angles is divided into two ranges, from +90° to 0° and from 0° to −90°. For the first range, both rectangular and semi-cylindrical cavities are oriented downward and the heated surface is on the top, hence suppression for the buoyancy force is taken place and Nu takes low values. From 0° to −90° the cavities are facing up and the buoyancy force is strong resulting in a higher heat transfer.

5. Conclusions

The work presents heat transfer results for rectangular and semi-cylindrical cavities. Smooth as well rough semi-cylindrical cavities were tested. The data is collected for 13 different inclination angles ranging from 90° (when the cavity is facing down) to −90° (when the cavity is facing up). Both cavities have the same surface area and the same heat flux.

The semi-cylindrical cavity shows higher values of Nusselt numbers than that of rectangular cavity at the same inclination angle. This increase ranges from 50 to 200% depending on the inclination angle. Minimum Nusselt number occurs when the cavities are facing down. The buoyancy-driven flow gets stronger when the inclined angle decreases resulting in higher Nusselt number. The initial inclination of the cavity from 90° to 0° causes a significant increase in average heat transfer rate, but a further increase in inclination angle appears to cause a small increase in average heat transfer rate.

It is observed that the presence of roughness delays the onset of convection motion at small deviation from the 90° angle. Therefore the heat transfer is more for the smooth cavity in this range. Beyond this range, the roughness element increases the heat transfer rate. At low tilt angle molecular conduction is the dominant mechanism of heat transfer; roughness seems to slow down the heat transfer mechanism by adding more form drag to the momentum of the flow. When the cavity is placed in an upward position, high convection current occurs. Roughness helps to trip the boundary layer and adds more turbulence to the flow resulting in increase in heat transfer.

References

[1] D. Angirasa, M.J.B.M. Pouriquie, F.T.M. Nieuwstadt, Numerical study of transient and steady laminar buoyancy-driven flows heat transfer in a square open cavity, Numer. Heat Transfer A 22 (1992) 223–239.
[2] D. Angirasa, I.G. Eggels, F.T.M. Nieuwstadt, Numerical simulation of transient natural convection from an isothermal cavity open on a side, Numer. Heat Transfer A 28 (1995) 755–768.
[3] ASME, Measurement uncertainty, ASNI/ASME PTC 19.1—1985 Part 1 (1996).
[4] A. Bouhdjar, A. Benkhelifa, Numerical study of transient mixed convection in a cylindrical cavity, Numer. Heat Transfer A 31 (1997) 305–324.
[5] W. Chakroun, M.M. Elsayed, S.F. Al-Fahed, Experimental measurements of heat transfer coefficient in a partially/fully open tilted cavity, ASME J. Solar Engrg. 119 (1997) 298–303.
[6] Y.L. Chan, C.L. Tien, Laminar natural coin shallow open cavities, ASME J. Heat Transfer 108 (1986) 305–309.
[7] K.S. Chen, J.A.C. Humphrey, F.S. Sherman, Experimental investigation of thermally driven flow in open cavities of rectangular cross-section, Philos. Trans. Roy Soc. London A 316 (1985) 57–84.

[8] H.W. Coleman, W.G. Steele, Experimental and Uncertainty Analysis for Engineers, Wiley, New York, 1989.
[9] M.L. Doria, A Numerical Model for the prediction of two dimensional unsteady flows of multi-component gases with strong buoyancy effects and recirculation, Notre Dame Report, TR-37191-74-4, 1974.
[10] M.M. Elsayed, Infiltration load in cold rooms, HVAC&R Res. 4 (2) (1998) 79–202.
[11] M.M. Elsayed, W. Chakroun, Effect of aperture geometry on heat transfer in tilted partially open cavities, J. Heat Transfer 121 (1999) 819–827.
[12] U. Gross, R. Spindler, E. Hahne, Shape-factor equations for radiation heat transfer between plane rectangular boundaries, letter in Heat Transfer 8 (1981) 219–227;
reported in J.R. Howel, Catalog of Radiation Configuration Factor, McGraw-Hill, New York, 1982.
[13] C.F. Hess, R.H. Henze, Experimental investigation of natural convection losses from open cavities, ASME J. Heat Transfer 106 (1984) 333–338.
[14] S.-S. Hsieh, M.-Y. Wen, Numerical computation of thermocapillary-driven convection in an open cylindrical cavity with different aspect ratios, Internat. J. Heat and Mass Transfer 36 (18) (1993) 4351–4363.
[15] H.R. Jacobs, W.E. Mason, W.T. Hikida, Natural convection in open rectangular cavities, in: Proc. Fifth Internat. Heat Transfer Conf., Tokyo, Japan, Vol. 3, 1974, pp. 90–94.
[16] H.R. Jacobs, W.E. Mason, Natural convection in open rectangular cavities with adiabatic side walls, Heat Transfer Fluid Mech. Inst. (1976) 33–46, Stanford University Press, Standford.
[17] P. Le Quere, J.A.C. Humphrey, F.S. Sherman, Numerical calculation of thermally driven two-dimensional unsteady laminar flow in cavities of rectangular cross section, Numer. Heat Transfer 4 (1981) 249–283.
[18] C.X. Lin, M.D. Xin, Transient Turbulent free convection in an open cavity, Inst. Chemical Engrg. Sympos. Ser. 1 (1992) 515–521.
[19] M. Miyamoto, T.H. Keuhn, R.J. Goldstein, Y. Katoh, Two dimensional laminar natural convection heat transfer from a fully or partially open square cavity, Numer. Heat Transfer A 15 (1989) 411–430.
[20] F. Penot, Numerical calculation of two dimensional natural convection in an isothermal open cavities, Numer. Heat Transfer 5 (1982) 421–437.
[21] M. Ruhul Amin, Natural convection heat transfer and fluid flow in an enclosed cooled at the top and heated at the bottom with roughness elements, Internat. J. Heat Mass Transfer 36 (10) (1993) 2707–2710.
[22] M. Sakata, Numerical study of natural convection in a cylindrical cavity bounded by a partially heated vertical wall, Fluid Dynamics Res. 18 (1993) 223–235.
[23] V. Sernas, I. Kyriakides, Natural convection in an open cavity, in: Proc. Seventh Internat. Heat Transfer Conf., Vol. 2, Munchen, Germany, 1982, pp. 275–286.
[24] R.A. Showole, J.D. Tarasuk, Experimental and Numerical studies of natural convection with flow separation in upward-facing inclined open cavities, Trans. ASME 115 (1993) 592–605.
[25] K. Vafai, J. Ettefagh, The effects of sharp corners on buoyancy-driven flows with particular emphasis on outer boundaries, Internat. J. Heat Mass Transfer 33 (10) (1990) 2311–2328.